



1 **Historical climate extremes in Europe and the connection between spring**  
2 **precipitation and summer heat**

3

4 *Laura Lipfert<sup>1,2</sup> Ralf Hand<sup>1,2,3</sup>, Angela-Maria Burgdorf<sup>1,2</sup>, Christian Pfister<sup>1,4</sup>, Heinz Wanner<sup>1,2</sup>, and*  
5 *Stefan Brönnimann<sup>1,2,\*</sup>*

6 <sup>1</sup> Institute of Geography, University of Bern, Bern, Switzerland

7 <sup>2</sup> Oeschger Centre for Climate Change Research, University of Bern, Bern, Switzerland

8 <sup>3</sup> Deutscher Wetterdienst DWD, Offenbach, Germany

9 <sup>4</sup> Institute of History, University of Bern, Bern, Switzerland

10 \* Corresponding author: stefan.broennimann@unibe.ch

11

12 **Abstract**

13 Hot European summers are often preceded by dry springs such as in 2022, but also in 1473 or 1540, two well-  
14 known summers of catastrophic heat. Spring precipitation deficits deplete soil moisture levels, which can  
15 amplify extreme summer temperature anomalies in Europe through land-atmosphere feedback mechanisms and  
16 altered atmospheric circulation. However, the link is not particularly strong, and hence long time series might  
17 help to better elucidate the mechanisms. Starting from documentary data and an atlas of temperature,  
18 precipitation, and atmospheric circulation over Europe for climate extremes in the last 600 years, we explore  
19 this relationship in more detail. We analyse the extreme heat summer of 1473, which followed dry spring  
20 conditions in Southeastern Europe related to a positive East Atlantic pattern. We then use the ModE-RA paleo-  
21 reanalysis and combine it with an analysis of 11,760 years of atmospheric model simulations as well as other  
22 reanalyses and reconstructions. Using a moving climatology approach with LOESS regressions to calculate  
23 anomalies, we identify significant negative correlations between winter-spring precipitation and summer  
24 temperatures in all data sets in the latitude band 36°-48° N (strongest over southeastern Europe), corresponding  
25 to known moisture-limited regions. Moreover, apart from precipitation anomalies, hot summers are preceded by  
26 increased blocking over north-central Europe and a positive East Atlantic pattern. Conversely, dry winter-  
27 springs are followed by more frequent blocking over northern Europe and, in model simulations, an increase in  
28 frequency and intensity of summer heatwaves. A linear regression approach for temperature in the northern  
29 Mediterranean region shows that precipitation in April and May has a strong, direct influence that does not  
30 vanish when taking the detailed atmospheric circulation in winter, spring, and summer into account, and hence  
31 cannot be explained by the effect of circulation on both, spring precipitation and summer temperature.

32

33



## 34 **1 Introduction**

35 Some of the hottest recent European summers, such as 2022, were preceded by dry springs. In fact,  
36 spring precipitation deficits play a crucial role in establishing conditions for summer heat extremes in  
37 Europe, primarily by influencing soil moisture levels (see review by Seneviratne et al., 2010).  
38 Reduced spring rainfall depletes soil moisture, which limits evaporative cooling during the summer  
39 and thereby amplifies summer temperature extremes (Vautard et al., 2007; Fischer et al., 2007;  
40 Seneviratne et al., 2010; Rousi et al., 2023; Böhnisch et al., 2024). These feedback mechanisms are  
41 particularly prominent in Southern Europe, where soil moisture is often a limiting factor for  
42 evapotranspiration, creating conditions favorable to heatwaves that can then propagate northward into  
43 Central Europe through atmospheric circulation patterns (Vautard et al., 2007; Fischer et al., 2007;  
44 Pardo et al., 2024).

45 Several studies have analyzed the relationship between spring precipitation and summer heat  
46 extremes in Europe, employing various methods to explore the mechanisms. Many studies rely on  
47 model simulations to quantify the contributions of land-atmosphere coupling and soil moisture  
48 dynamics and explore the potential evolution of these mechanisms under varying climatic conditions  
49 (Seneviratne et al., 2010; Quesada et al., 2012; Rousi et al., 2023; Böhnisch et al., 2024). Other  
50 studies utilize observational data of the past to explore these relationships over specific time frames,  
51 for example, by analyzing observations from meteorological stations in central and southeastern  
52 Europe (Hirschi et al., 2011) or by using reanalysis products (Quesada et al., 2012; Träger-Chatterjee  
53 et al., 2013) to examine soil moisture's impact on heat extremes. However, due to data limitations,  
54 most studies with observational data do not extend beyond the mid-20th century.

55 One exception is the study by Wang et al. (2011) that analyzed observational data spanning 1901  
56 to 2005 to examine the connection between winter and early spring precipitation deficits and summer  
57 heat extremes in Europe. Their findings highlight how these precipitation deficits, modulated by the  
58 North Atlantic Oscillation (NAO), influence soil moisture states, subsequently affecting summer  
59 temperature variability and drought severity, particularly in the Mediterranean region.

60 There are, however, several well-documented cases of spring precipitation deficits followed by  
61 summer heat in earlier centuries, most notably the year 1540 (Lipfert et al., 2026). At the same time,  
62 there are equally interesting exceptions of hot summers following wet springs (such as in 2024).  
63 Analyzing these years as case studies, as well as statistically, could furthermore contribute to a better  
64 understanding of present and future summers. A recent publication by Pfister and Wanner (2021)  
65 discusses climatically extreme seasons in Europe (cold/warm, wet/dry) of the last 1000 years with  
66 respect to their impacts. The recent ModE-RA paleo-reanalysis dataset family (Valler et al., 2024)  
67 allows producing an "Atlas of European climate extremes since 1421", which is the supplement to  
68 this article, comprising maps of temperature, precipitation, sea-level pressure (SLP), and 500 hPa  
69 geopotential height (GPH) anomalies for a total of 107 described extreme seasons (Pfister and



70 Wanner, 2021) that overlap with ModE-RA. We use this atlas as a starting point and select suitable  
71 case studies, as all seasons in the atlas are well covered with documentary data. Then we use the  
72 entire 600-year time period and combine the ModE-RA products with other reconstructions and  
73 reanalyses to explore the relationship between dry springs and hot summers in Europe in more detail.  
74 Using documentary sources, we extend the time period even further back, to the early 14<sup>th</sup> century.  
75 Our approach not only extends the temporal scope, allowing analyses of hydroclimate and  
76 atmospheric circulation over the past 600 years, but also provides empirical evidence for the  
77 mechanisms driving these relationships, offering new insights into past climate variability and its  
78 relevance for understanding future risks.

## 79 **2 Data & Methods**

### 80 **2.1 Climate data and simulations**

81 To analyze spring precipitation and summer temperatures across Europe, we use seasonal means from  
82 ModE-RA, a 20-member global gridded monthly paleo-reanalysis spanning the period from 1421 to  
83 2008, with a horizontal resolution of approximately 1.8° by 1.8° (T63) (Valler et al., 2024). The  
84 reanalysis integrates an ensemble of transient model simulations (ModE-Sim; Hand et al.; 2023) and  
85 observational data using an offline data assimilation approach (Valler et al., 2024). Assimilated  
86 climate information includes natural proxies, documentary records, and instrumental measurements.

87 We further analyze a 20-member ensemble of the underlying atmospheric simulations ModE-Sim.  
88 The simulations are performed using the ECHAM6 general circulation model. The model utilizes ten  
89 distinct realizations of HADISST2 (Titchner and Rayner, 2014) in addition to ten of their  
90 recombinations as boundary conditions for sea-surface temperature (SST) and sea ice from 1850 on.  
91 Before 1850, the ensemble relies on SST reconstructions by Samakinwa et al. (2021). Radiative and  
92 volcanic forcings follow the standard PMIP4 protocol (Jungclaus et al., 2017), while land-surface  
93 conditions for ECHAM6 are provided by the JSBACH integrated land-surface model.

94 Alongside ModE-RA and ModE-Sim, we investigate ModE-RAclim, an alternative version of ModE-  
95 RA that uses 100 randomly selected years from the ModE-Sim ensemble to generate the prior state,  
96 thereby improving covariance estimation. With this approach, the prior and covariance structure are  
97 time-invariant. Thus, any time variation in ModE-RAclim results solely from assimilated  
98 observations, not from model boundary conditions. In contrast, ModE-RA uses 20 distinct transient  
99 members of ModE-Sim, retaining the impact of boundary conditions (Valler et al., 2024).

100 In addition to the ModE dataset family, we also used the reanalysis datasets ERA5 (Hersbach et al.,  
101 2020) and 20CRv3 (Slivinski et al., 2019). The latter two were used to calculate atmospheric  
102 blocking. The Tibaldi-Molteni algorithm (Tibaldi and Molteni, 1990) was applied to ERA5 and all 80  
103 members of 20CRv3 (see Rohrer et al., 2020, for details). Further, we used a reconstruction of  
104 seasonal mean Tibaldi-Molteni blocks that extends back to 1728 and is based on the seasonal



105 frequencies of reconstructed daily weather types (Pfister et al., 2025). The blocking reconstruction is  
106 described in more detail by Brönnimann et al. (2025).

## 107 **2.2 Documentary data**

108 Investigating dry springs in the pre-instrumental period requires specific evidence. Prior to the early  
109 16<sup>th</sup> century, this mainly includes narrative reports, such as “the spring was dry”, occasionally  
110 including observed impacts of droughts on pastures. In the English countryside, spring was perceived  
111 as an event rather than a season. Summer began when the growing season started, i.e., at a variable  
112 date in April or May. It lasted until the harvest season, autumn, in August and September (Pribyl and  
113 Cornes, 2020). From 1500, estimated spring precipitation is available for the Czech Lands  
114 (Dobrovolný et al., 2014) and for other countries increasingly in the form of the number of rain days  
115 obtained from weather diaries. From 1665, monthly rainfall is documented for Paris (Pliemon et al.,  
116 2023; Slonosky, 2002). Continuous evidence on hot summers is obtained from proxy data such as  
117 grape harvest dates (Labbé et al., 2019), evidence of wine-must quality (Pfister et al., 2024), and  
118 wine-must yields (Pfister et al., 2026). Information on summer droughts is mainly based on observed  
119 duration of periods without effective rain, low river levels, and drying up of springs. A considerable  
120 amount of evidence comes from the Euro-Climhist database (Pfister et al., 2017,  
121 [www.euroclimhist.unibe.ch/](http://www.euroclimhist.unibe.ch/)). Seasonal temperature indices are available from the late 12<sup>th</sup> century  
122 (<https://boris.unibe.ch/191962/>) but are currently being revised.

## 123 **2.3 Methods**

### 124 2.3.1 Atlas

125 The “Atlas of European climate extremes since 1421” (Electronic Supplement) shows maps of  
126 anomalies relative to the period 1500-1900 for the ensemble means of 2 m temperature, 500 hPa GPH  
127 (overlaid contours), precipitation, and SLP (overlaid contours). Each season includes these four fields  
128 for all three data sets (ModE-RA, ModE-RAclim, ModE-Sim). All maps of all seasons and all data  
129 sets are shown on the same color scale and contour spacing. Note that maps for other seasons, for all  
130 four variables and all three data sets can conveniently be generated in ClimeApp (Warren et al.,  
131 2024). The documentary sources listed in the Appendix complement the Atlas maps.

### 132 2.3.2 Seasonal precipitation and temperature

133 For the analysis, we calculate seasonal anomalies in ModE-RA, ModE-RAclim, and ModE-Sim using  
134 a moving climatology. For this, we apply a LOESS (Locally Weighted Scatterplot Smoothing)  
135 algorithm (Cleveland, 1979). This method performs a series of localized linear regressions. The  
136 smoothing parameter is selected to correspond to a moving window of approximately 31 years. A key  
137 advantage of using LOESS regression is its ability to include data from both the beginning and end of  
138 the time series. Consequently, we have more seasons to analyze, and this enhances our ability to  
139 investigate the relationship between dry springs and hot summers in Central and Southern Europe.



140 Seasonal anomalies were calculated for January–May (JFMAM, Jan and Feb were included since part  
141 of the area has snow in winter, which might contribute to spring moisture), total precipitation, and  
142 June–August (JJA) 2m temperature. This approach, using a moving climatology to calculate the  
143 anomalies, enables the comparison of temperature and precipitation anomalies across different  
144 centuries, providing a robust framework for historical climate analyses. Note that the LOESS  
145 approach was applied to all variables, fields and indices used in this paper, except when stated  
146 otherwise.

147 The geographical definitions of the European regions used in this study were based on the IPCC 6th  
148 Assessment Report (IPCC, 2021). These standardized regional definitions ensure comparability with  
149 previous research and consistency in defining climate patterns across different time periods.

150 We then performed a composite analysis in which we analyzed the relation between JFMAM  
151 precipitation and JJA temperature forward and backward, i.e., we calculated composites of 2 m  
152 temperature for all summers following very dry springs (i.e., JFMAM precipitation anomalies below  
153 the 10<sup>th</sup> percentile). Conversely, we plotted composite maps for JFMAM precipitation that preceded  
154 hot summers (2 m temperature anomalies above the 90<sup>th</sup> percentile). For these composite analyses, all  
155 members and years from the ModE-RA reanalysis dataset were included separately. We also  
156 calculated respective composites for the six circulation indices described in the next section.  
157 Statistical testing of the composites was performed with a t-test.

### 158 2.3.3 Atmospheric circulation

159 To address atmospheric circulation, we analyzed, in addition to fields of 500 hPa GPH and SLP,  
160 atmospheric circulation indices, derived from ModE-RA data. These comprise three indices based on  
161 SLP: the NAO (difference between 9° W/40° N and 22.5° W/64° N), the East Atlantic pattern (EA,  
162 30° E/55° N minus 20° W/55° N), and the Scandinavian pattern (SCA: 15° E/40° N minus 30° E/64°  
163 N). In addition, three indices of the jet stream over the Atlantic–European sector describing the  
164 strength, tilt, and latitude (STR; TIL, LAT) of the jet at 500 hPa were used (for details see  
165 Brönnimann et al. 2025). Note that while the latter indices are close to mutually independent, the  
166 former are not (NAO is correlated with SCA), and the former and the latter are correlated, i.e., NAO  
167 is correlated with STR ( $r = 0.19$  to  $0.61$  depending on the season), EA with TIL ( $-0.69$  to  $-0.71$ ), and  
168 SCA with LAT ( $-0.15$  to  $0.51$ ). However, with these six indices, we hope to capture circulation effects  
169 on temperature and precipitation rather comprehensively. All indices were calculated based on (non-  
170 standardised) anomalies from the long-term (1421–2008) mean seasonal cycle.

171 We then used a regression approach to predict JJA 2 m temperature from spring predictors. In  
172 addition to monthly precipitation in (Jan. to May) and the six atmospheric circulation indices (each for  
173 Jan–Feb and Mar–May), the predictors included 2 m temperature anomalies in the Western North  
174 Atlantic (35–55° N, 70–40° W, Mar–May, identified to be linked to European heatwaves in Lipfert et  
175 al., 2024) as well as in the NINO3.4 region (May) and global mean Aerosol Optical Depth at 550 nm



176 in the 12 preceding months (Jun-May) from PMIP4 (Jungclauss et al., 2017) and Sato et al. (1993).  
177 The latter series is the only one that we did not filter with a LOESS filter. Note that the same  
178 stratospheric aerosol data were also used in ModE-Sim, which forms the basis of ModE-RA. A  
179 second regression model included the six circulation indices for JJA.

#### 180 2.3.4 Blocking and heatwaves

181 Further, we analyzed composites of atmospheric blocking in the same way as temperature and  
182 precipitation, i.e., the blocking frequency in summers following dry springs and in springs preceding  
183 hot summers. However, as blocking is not included in ModE-RA, we used three different, shorter  
184 blocking data sets: reconstructions back to 1728 (Brönnimann et al., 2025), 20CRv3 back to 1806, and  
185 ERA5 back to 1940. For consistency, the list of dry springs and hot summers for all data sets was  
186 calculated from the ensemble mean of ModE-RA.

187 Finally, we also analyzed JJA heatwaves to assess their relationship with spring precipitation  
188 anomalies. In a previous paper, we thoroughly tested the ability of the ensemble of atmospheric  
189 simulations ModE-Sim to simulate heatwave variability across the Northern Hemisphere (Lipfert et  
190 al., 2024). The heatwave definition we use follows the standard heatwave definition requiring a  
191 minimum of three consecutive days exceeding a 90th percentile threshold based on an 11-day moving  
192 window and a 31-year running mean climatology (Lipfert et al., 2024; note that this is comparable to  
193 the LOESS approach). Seasonal heatwave characteristics were calculated for JJA and correlated with  
194 JFMAM precipitation anomalies for 1420-2003 (1436-1993 due to the 31-year running average).

### 195 3 Results

#### 196 3.1 Case studies

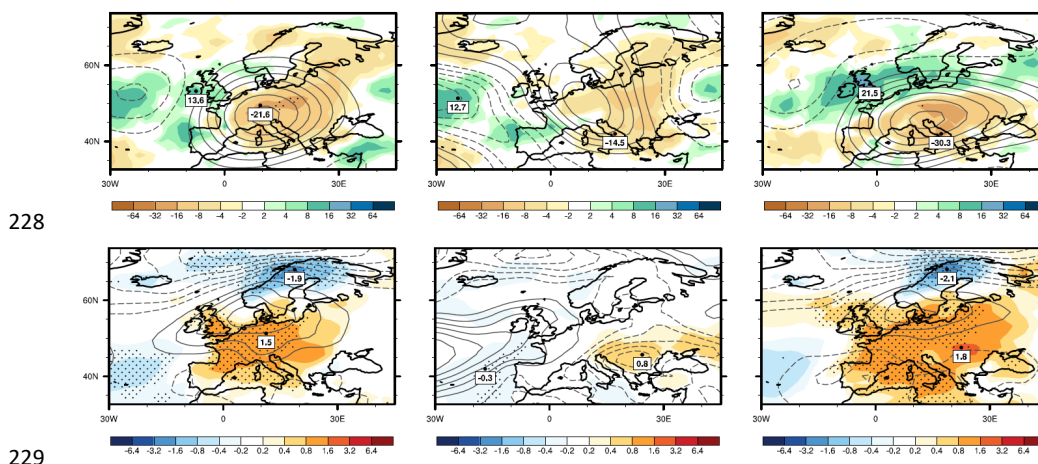
197 Before delving into the statistical analysis of climate data, it is worth summarizing the documentary  
198 sources for the hot summers that follow dry springs. Pfister and Wanner (2021) give detailed  
199 information on 14 hot summers in Central Europe after 1421 (1471, 1473, 1536, 1540, 1545, 1556,  
200 1590, 1616, 1666, 1684, 1706, 1719, 1859, 1947), which are therefore included in the Atlas. Further  
201 summers prior to 1421 can be added. In total, 22 years were classified; detailed descriptions of all of  
202 them are given in the Appendix. In 9 years (1304, 1361, 1393, 1473, 1504, 1516, 1540, 1706, and  
203 1719), a dry spring was followed by summer heat and drought. In the 4 years 1375, 1503, 1536, and  
204 1684, the spring drought preceding the summer drought was limited to May. In the three years 1590,  
205 1616, and 1947, the summer heat and drought were shifted in time. Evidence of a relationship  
206 between dry springs and dry summers is thus found in 16 of the 22 cases. The dry springs in 1420,  
207 1559, 1603, 1638, and 1686 were not followed by a very dry summer, and in 1326, the relationship is  
208 uncertain.

209 The most prominent examples of very hot summers preceded by dry springs are 1473 and 1540,  
210 with 1473 showing the longest duration and greatest geographical extent. In a previous article on



211 extreme summers (Lipfert et al., 2026), we analyzed 1540 and 1590, though not in relation to spring  
 212 precipitation. We found that both were associated with positive 500 hPa GPH anomalies arguably  
 213 linked to omega (1540) or dipole (1590) blocking patterns, but differed clearly in temporal  
 214 development. Here we analyze the case of 1473 in more detail, as it was among the most extreme  
 215 summers of the past 600 years. In fact, Cook et al. (2022) describe the period 1400-1480 in Europe as  
 216 a “megadrought”.

217 Documentary sources (see Appendix) describe an extremely dry year in a region stretching from  
 218 France to Russia. Rivers dried out and fires ravaged. The dryness lasted until early the next winter and  
 219 was followed by locust invasion in 1474. Anomaly maps of temperature and 500 hPa GPH in JJA, as  
 220 well as precipitation and SLP in spring of 1473 (here we show the climatological spring season,  
 221 MAM, as in Pfister and Wanner, 2021) are shown in Fig. 1 from the “Atlas”. The summer was hot  
 222 throughout central Europe, extending east and west. Scandinavia was cold, and southern Europe was  
 223 near normal. A large 500 hPa GPH anomaly was centered over Germany. We find a slightly stronger  
 224 (in 18 out of 20 members), less tilted (i.e., more zonal, 20 out of 20), and poleward shifted jet (20 out  
 225 of 20) over the Atlantic European sector. The preceding spring shows a negative precipitation  
 226 anomaly over Central and Eastern Europe. The SLP anomaly shows a distinct positive EA pattern. In  
 227 fact, the EA index was positive in 19 out of 20 members.



228 **Figure 1:** (top) MAM 1473 total precipitation (mm) and SLP anomalies (contour lines) as well as (bottom) JJA  
 231 1473 2-m temperature and 500hPa GPH anomalies (contour lines) for (left) ModE-RA, (middle) ModE-Sim,  
 232 and (right) ModE-RAclim. Contour distance is 1 hPa for SLP and 10 GPH for 500 hPa GPH (negatives dashed,  
 233 zero not shown). Stippling indicates where at least 15 out of 20 members agree in sign. Minima and maxima in  
 234 temperature and precipitation are indicated.

235 The comparison between ModE-RA, ModE-RAclim, and ModE-Sim shows that the largest part of the  
 236 temperature signal stems from the assimilated observations. This is indicated by the fact that ModE-  
 237 RA and ModE-RAclim are very similar. However, there is also a forced component (i.e., the signal



238 arising from model boundary conditions, which arguably largely stems from volcanic aerosols and  
239 SSTs), and there is also similarity between ModE-Sim and ModE-RAclim, even though they are  
240 mutually independent. ModE-Sim shows a similar spring precipitation anomaly with the largest  
241 deficits over south-eastern Europe. There is also a slightly positive EA pattern in spring in ModE-Sim,  
242 similar to that in ModE-RAclim and ModE-RA.

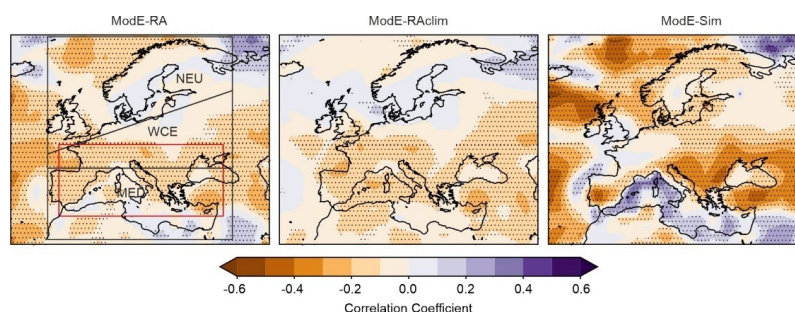
243 In the following, we analyze the relations statistically and test, e.g., whether the EA pattern is a  
244 frequent precursor of hot summers and whether the spatial shift (the dry area in spring is farther east  
245 than the hot area in summer) is a recurring feature.

### 246 **3.2 Correlations across Europe**

247 To investigate the link between spring precipitation deficits and summer heat extremes across Europe,  
248 we first examined grid-point-based Pearson correlations between JFMAM precipitation anomalies and  
249 JJA 2 m temperature anomalies calculated using the LOESS approach. This analysis was done for  
250 ModE-RA, Mode-RAclim, and ModE-Sim, for each ensemble member.

251 The spatial correlations in ModE-RA reveal significant regional variability across Europe (Fig. 2).  
252 Correlations are negative in a band stretching ca. 36–48° N, indicating a general tendency for drier  
253 springs to be associated with hotter summers. Although significant, the correlations are around -0.2 or  
254 slightly weaker. Correlation is near zero in northern Europe. This suggests that spring precipitation  
255 plays no significant role in modulating summer heat extremes in Northern Europe, likely due to  
256 weaker land-atmosphere interactions and lower evapotranspiration sensitivity, as supported by Hirschi  
257 et al. (2011). We therefore do not consider the IPCC region “Northern Europe” further. The  
258 significant correlations in West Central Europe (WCE) and the Mediterranean (MED) indicate an  
259 association between spring precipitation deficits and summer heat extremes, consistent with the  
260 region’s strong land-atmosphere coupling identified in prior studies (Seneviratne et al., 2010). In  
261 several areas (e.g., the Mediterranean), we see a land-sea gradient. However, by analyzing correlation  
262 coefficients, we can capture only linear relationships and with the grid-point-based approach, we  
263 investigate only co-located spring precipitation deficits and hot summer temperatures. To address  
264 these issues, we conducted composite analyses.

265 Correlations in ModE-RAclim are similar to those in ModE-RA, whereas in the pure model  
266 simulations (ModE-Sim) without observation input, they are somewhat stronger and positive over the  
267 Mediterranean Sea. This comparison shows that the signal in ModE-RA is largely observation-driven.  
268 In the following, we show results only for ModE-RA, except for the heatwave analysis (and we  
269 exclude the ocean surface from the interpretation). As ModE-RA and ModE-RAclim are monthly data  
270 sets, heatwaves can only be analyzed in ModE-Sim.



271

272 **Figure 2.** Gridpoint-based correlations between JFMAM precipitation anomalies and JJA 2m temperature  
 273 anomalies for (left) ModE-RA, (middle) ModE-RAclim, and (right) ModE-Sim, 1421-2008. Stippling indicates  
 274 significance at the 95% confidence level. The left figure shows the IPCC regions NEU, WCE, and MED. The  
 275 red rectangle shows the region used for the regression approach.

### 276 3.3 Composite analysis

#### 277 3.3.1 Temperature and precipitation

278 We analyze composites of ModE-RA JFMAM precipitation anomalies of all years for which the JJA  
 279 temperature anomalies exceed the 90th percentile (Fig. 3) as well as composites of JJA 2 m  
 280 temperature anomalies for all years where JFMAM precipitation falls below the 10th percentile (Fig.  
 281 4) for three specific regions (entire Europe, Western-Central Europe, and the Mediterranean). Recall  
 282 that the analysis is performed per member, thus comprising  $20 \times 588 = 11,760$  years (which, however,  
 283 are not entirely independent). The 10<sup>th</sup> percentile thus corresponds to 1176 years per region. However,  
 284 the Euler diagrams show significant overlap among the selected cases across the three regions.

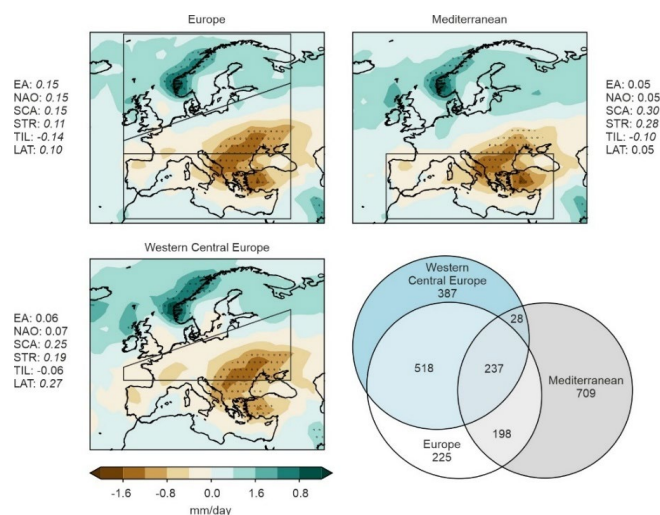
285 Before looking at spatial maps, it is interesting to note that, for Europe, 15% of the selected hot-  
 286 summer years were also dry-spring years; for Western Central Europe, the number is 17%, and for the  
 287 Mediterranean, even 23%. Hence, the association is strongest in the Mediterranean.

288 Analyzing the reconstructed fields, we find that precipitation in JFMAM in years with hot summers  
 289 tends to be anomalously low in South-Eastern Europe but wet in Norway. Both signatures are  
 290 statistically significant. The core region of precipitation deficit exhibits an amplitude of 1.4 mm/day.  
 291 The differences between the regions for which the temperature percentile is taken (Europe, WCE, and  
 292 MED) are small, consistent with the large overlap in selected cases. For the region Europe, we find  
 293 significant changes in atmospheric circulation, such as a positive EA pattern (similar to that in 1473),  
 294 NAO, SCA, and TIL. The signs are the same for WCE and MED, though generally less significant.  
 295 WCE is more closely associated with SCA, whereas MED is more closely associated with LAT.

296 Composites for 2 m temperature in summers following dry springs (Fig. 4) again show very similar  
 297 spatial patterns, with significant warming (approaching 1 K) centered over South Eastern Europe and  
 298 extending east and west. In contrast to the JFMAM precipitation composite, the JJA 2 m temperature  
 299 composite shows a land-sea contrast over the Mediterranean, although cooling is nowhere significant.

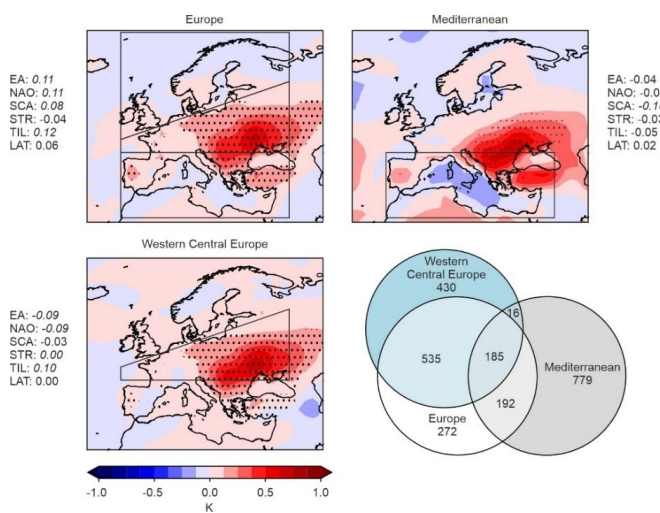


300 Dry springs are followed by negative EA, NAO, and SCA, thus a sign change in all three indices with  
 301 respect to springs preceding hot summers. No clear results are found for jet indices.



302

303 **Figure 3.** Composites of ModE-RA JFMAM precipitation anomalies for all years and ensemble members with  
 304 JJA 2m temperature >90<sup>th</sup> percentile in Europe, MED and WCE. Stippling indicates precipitation anomalies  
 305 larger than two standard deviations. The averages of the six circulation indices, here standardised for better  
 306 intercomparison are also indicated ( $p < 0.05$  in italics). The lower right shows an Euler diagram of the number  
 307 of cases.



308

309 **Figure 4.** Composites of ModE-RA JJA 2m temperature anomalies for all years and ensemble members with  
 310 JFMAM precipitation <10<sup>th</sup> percentile in Europe, MED, and WCE. Stippling indicates 2m temperature  
 311 anomalies exceeding two standard deviations. The averages of the six circulation indices, here standardised for  
 312 better intercomparison are also indicated ( $p < 0.05$  in italics). The lower right shows an Euler diagram of the  
 313 number of the cases.

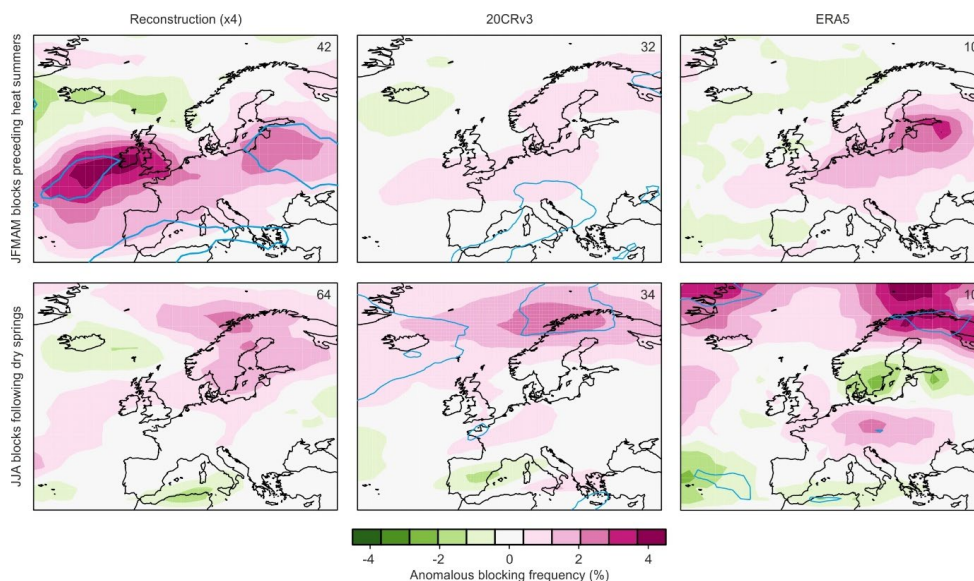


314 The plots confirm that there is a relation between summer temperature and winter-spring  
 315 precipitation, both when analyzing forward or backward. All composites identify Southeastern Europe  
 316 as the region showing the most pronounced effects. We expect this effect to be strongest in regions  
 317 where evaporation is moisture-limited (McVicar et al., 2012), and this is indeed the case. The affected  
 318 area is independent of the study region that we choose for the composites.

### 319 3.3.2 Atmospheric circulation and blocking

320 To better address the atmospheric circulation involved in the coupling, we analyzed blocking  
 321 frequency. Given the overlap among the selected cases, we analyzed only the region of Europe. Three  
 322 different data sets are analyzed: a statistical reconstruction back to 1728, 20CRv3, and ERA5. Note  
 323 that the first of these data sets has large uncertainties but covers most events. The second is clearly  
 324 less reliable than ERA5, but is also longer. The consistency between the analyses of the three data sets  
 325 nevertheless allows some conclusions.

326 The analysis (Fig. 5) shows that JFMAM blocking frequency preceding hot summers tends to be  
 327 higher in an area stretching from West of Ireland to the Baltic states, i.e., at the southern flank of the  
 328 storm track extension. This imprint is typical for a poleward-shifted jet (Brönnimann et al.; 2025).  
 329 Conversely, JJA blocking frequency following dry JFMAM is increased in northern Scandinavia. A  
 330 secondary maximum over Central Europe is only marginally or not significant.



331

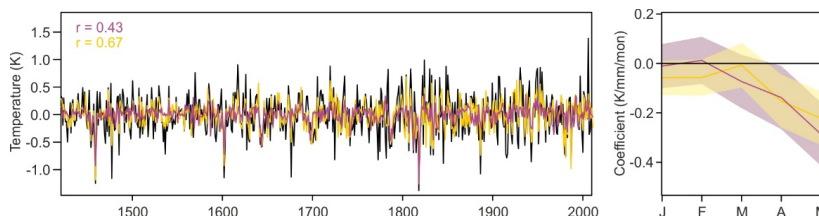
332 **Figure 5.** Anomalies in blocking in JFMAM preceding heat summers in Europe (top) and in JJA following dry  
 333 springs in Europe (bottom) in three different data sets (left to right). Blue lines indicate significant ( $p < 0.05$ , t-  
 334 test) anomalies. Numbers in the top left indicate the spatial average of blocking (italics indicate significance),  
 335 and the number of cases is indicated in the top right.



336 **3.4 Regression analysis**

337 Is the spring-summer link really due to precipitation, or could atmospheric circulation alone explain it  
 338 by driving both, the precipitation deficit in spring and the heat in summer? To test this, we focused on  
 339 the identified region with the strongest correlation, namely 8° W-38° E, 38-48° N. We further  
 340 considered only land grid cells and computed regional averages of precipitation (here treating Jan-  
 341 May as separate months) and JJA 2 m temperature, which is the predictand. Further explanatory  
 342 variables were chosen to capture oceanic influences, volcanic eruptions, as well as atmospheric  
 343 circulation (all six atmospheric circulation indices, each for Jan-Feb and for Mar-May). We then  
 344 proceeded with a backward selection until all p-values were below 0.1, while keeping all five  
 345 precipitation series. In addition, we also performed the same procedure for a model that additionally  
 346 has all six atmospheric circulation indices for Jun-Aug to test whether spring precipitation arises as a  
 347 significant predictor even if summer atmospheric circulation is accounted for directly.

348 The two models were similar in terms of the variables retained from the preceding spring: these  
 349 included volcanic aerosols, the indices SCA and TIL, and either the NAO (spring model) or STR  
 350 (spring-summer model) in MAM. Some January-February indices were kept (NAO or TIL). In the  
 351 summer model, five summer circulation indices were kept. In terms of precipitation, April and  
 352 particularly May were significant in both models (January at  $p < 0.1$  in the spring-summer model). This  
 353 brief analysis shows that precipitation in late spring influences JJA temperature beyond what is  
 354 already captured in atmospheric circulation (neither spring nor summer).



355

356 **Figure 6.** Time series of JJA 2 m temperatures in the land area between 8° W and 38° E, 36-48° N in ModE-RA  
 357 (black) and predicted from the regression models based on spring-only predictors (purple) and spring-summer  
 358 predictors (orange). Right: Coefficients (95% confidence intervals shaded) for precipitation in January to May in  
 359 the two models.

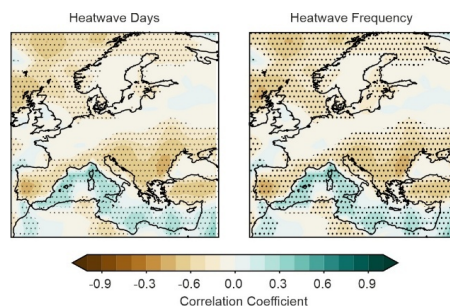
360 Observed and fitted JJA temperatures are shown in Fig. 6. The spring-only model explains 19% of the  
 361 variance ( $r = 0.43$ ), the spring-summer model 45% ( $r = 0.67$ ). Note that, although in the former model  
 362 all predictors lead the predictand, they are not fully independent, particularly in the early part of the  
 363 record; hence this result cannot be interpreted as indicating predictability. This is because seasonal  
 364 observations such as tree ring width or grape harvest dates are assimilated using a forward model that  
 365 may also include April or May temperatures (which in turn are influenced, e.g., by the NAO). Note  
 366 also that the AOD predictor is the same as that used to force the model, which is the basis of ModE-



367 RA, and that we use the ensemble mean which smoothes out variability. Hence, the 19% explained  
368 variance should not be confounded with a forecast skill.

### 369 3.5 Heatwave indices

370 Finally, we analyzed the connection between different heatwave indices and a spring precipitation  
371 deficit. For this, we use the heatwave characteristics calculated in Lipfert et al. (2024) and calculate  
372 them within ModE-Sim, the underlying atmospheric model simulations of ModE-RA. Results show  
373 the same pattern as for the seasonal means, i.e., negative correlations between heatwave days or  
374 frequency with winter-spring precipitation. As for the ModE-Sim seasonal results, the correlation  
375 reverses over the Mediterranean Seas, and it is somewhat stronger than for JJA temperature. Again,  
376 the moisture limited regions, and in particular, southeastern Europe show the strongest negative  
377 correlations.



378

379 **Figure 7.** Correlation between ModE-Sim Jan-May precipitation anomalies (with respect to a 31-year running  
380 mean) and June-August heatwave days and frequency. Hatching indicates significant correlations.

### 381 4 Discussion and Conclusion

382 We find a link between dry springs and warm summers in climate reconstructions, consistent with  
383 other studies. Based on documentary data, we find that 16 of 22 hot summers, were preceded by dry  
384 springs. Analyzing the momentous summer of 1473 in detail, we find not only a very dry spring but  
385 also specific features of spring atmospheric circulation (positive EA and SCA patterns, positive jet  
386 latitude) that are confirmed as typical in statistical analyses. This also concerns the shift in the area of  
387 hot summer with respect to the area of dry spring. At the same time, we also note that not all heat  
388 summers are preceded by a dry spring. Statistical analyses of ModE-RA showed overall rather weak  
389 gridpoint-wise correlations. Nevertheless, the signal is consistent across the family of ModE-RA  
390 products, i.e., it appears in the underlying model simulations (ModE-Sim), in a product constrained by  
391 observations alone (ModE-RAclim), and in the combination, the paleo-reanalysis ModE-RA.

392 Composite analyses confirm that hot summers (>90<sup>th</sup> percentile) are often preceded by drier-than  
393 normal springs and that dry springs (<10<sup>th</sup> percentile) are often followed by hotter-than normal  
394 summers. The region whose precipitation deficit affects Europe most strongly is southeastern Europe;  
395 in the correlation analysis, we found the strongest correlations in a latitude band between 36° and 48°



396 N. This corresponds well to the area where evaporation is moisture-limited. A regression analysis of  
397 land area temperature in this region confirms a link that is indeed driven by spring precipitation rather  
398 than arising from atmospheric circulation effects on both. Further, the analysis confirmed a result  
399 from the documentary data, namely that April, and particularly, May precipitation deficits have the  
400 largest effect on summer temperature. Also note that including summer atmospheric circulation in the  
401 analysis did not change the coefficients for April and May precipitation. Finally, the analysis of daily  
402 data sets shows that dry springs not only lead to hot summers but also to more intense heatwaves and  
403 more frequent blocking. As to possible precursors, the most consistent link to spring atmospheric  
404 circulation was to a positive EA pattern.

405 This work uses of an “Atlas of European Climate Extremes since 1421” which presents an analysis in  
406 of climatic extremes in ModE-RA, as discussed in detail in Pfister and Wanner (2021). The atlas is  
407 published as an electronic Supplement to this paper.

408 Although this study investigates a link between dry springs and hot summers, it should be pointed out  
409 that seasonal predictability was not the focus of the paper and, the results cannot be taken as a  
410 measure of it due to our experimental setup. Nevertheless, we think that a better understanding of this  
411 link is relevant to understanding past and present extreme events.

412 **Data availability:** The ModE-RA, ModE-RAclim, and ModE-Sim data (Valler et al., 2024) can be downloaded  
413 from DKRZ (<https://www.wdc-climate.de/ui/entry?acronym=ModE-RA>). ERA5 reanalysis data are available  
414 from the Copernicus Climate Change Service Data Store. NOAA/CIRES/DOE 20th Century Reanalysis (V3)  
415 data were provided by the NOAA PSL, Boulder, Colorado, USA, from their website at <https://psl.noaa.gov>.  
416 Euro-Climhist (Pfister et al., 2017) is available from <https://www.euroclimhist.unibe.ch/> (last access: 14 April  
417 2026). The blocking reconstructions (Brönnimann et al., 2025) are available from the BORIS Portal at  
418 <https://doi.org/10.48620/36384> (last accessed 19 April 2026)

419 **Funding:** The work was funded by the Swiss National Science Foundation project DVDW (grant no. 219746)  
420 and by the European Commission through H2020 (ERC Grant PALAEO-RA 787574).

421 **Acknowledgments:** The simulations underlying ModE-RA were performed at the Swiss National  
422 Supercomputing Centre (CSCS).

423



424 **Appendix: Documentary data for hot summers that followed dry springs**

425 All links indicated in this Appendix refer to the Euro-Climhist Database (Pfister et al., 2017).

426 **1304: Spring dry; summer hot and dry**

427 No winter frost was experienced in Mainz (DE) and in Wroclaw (PL) (Alexandre 1987; 428), A hot  
428 spring spurred vegetation growth. Ripe grapes were already found in Alsace in early July. Spring and  
429 summer were (almost) without rain. The period between April and July was extremely warm and dry.  
430 Most wells dried up and the Rhine could be crossed on horseback in several places between  
431 Strasbourg and Basel, just like on the Danube between Klosterneuburg and Krems, (AT). Large grape  
432 harvests of exceptional quality were gathered in Colmar, (FR) Metz (FR) and Rouen (FR). A second  
433 flowering of trees was observed in Tyrol, Austria, indicating hot conditions in September and October.  
434 The entire year was very warm. (Pfister and Wanner, 2021: 176).

435 **1326: Spring uncertain, summer hot and dry**

436 Paris (FR): No rain during four months in summer. No thunderstorm. Low level of rivers. Egmond  
437 (NL): no rain during summer. Caen (FR), Tournai (BE): Drying up of sources. Low level of rivers.  
438 (Alexandre, 1987: 443).

439 “Manorial accounts from the Bishopric of Winchester [...], in southeast England, and Norwich  
440 Cathedral Priory [...], primarily in Norfolk, pasture fell short everywhere, and this had severe  
441 repercussions for milk production; in Norfolk, trees withered in the dry conditions, and the harvest  
442 was very short” (Pribyl, 2017; Titow, 1960). “In 1326 [...].there was such a drought over all of  
443 England, in summer as in other times of the year, that men had to lead their livestock to water, in  
444 some parts of the country for three or four leagues [ca. 9–12 miles]. Wells and streams, cisterns and  
445 marshes dried out [...] The river Thames was for almost the whole year salty.” (Pribyl and Cornes,  
446 2019).

447 **1361: Spring dry; summer hot and dry**

448 Paris (FR): Spring very warm and very dry. Summer “tempéré”. Mainz (DE): Summer without any  
449 thunderstorm. Constance (DE), Liège (BE), and Wroclaw (PL): Heat and drought during the entire  
450 summer. Zwettl (AT): Parched soil. In Prussia grain was burning in the fields (Alexandre, 1987: 490;  
451 Buisman, 1996: 204). Winchester (UK): As a consequence of severe drought stress, the meadows did  
452 not produce a usable forage yield (Titow, 1970: 319). In England the spring-summer 1361 had the  
453 highest temperature in a reconstruction based on grain harvest dates for the period 1256–1431 (Pribyl  
454 et al., 2012; Pribyl, 2017).

455 **1375: May dry; summer hot and dry**

456 Mainly sunny and hot from May to August in Mainz (DE). At full maturity, the grapes were dried out.  
457 As in 1540, the start of the grape harvest was delayed until the next rainy period in mid-September,  
458 which was “useful for the grapes” Good grape harvest in Constance (DE) (Alexandre 1987: 514). In



459 Basel (CH) and Limburg an der Lahn (DE) the period was almost without rain for 14 weeks. A hot  
460 summer (including spring) and warm autumn were recorded in England (Pfister and Wanner, 2021:  
461 177).

462 **1393: Spring dry; summer hot and dry**

463 The drought started in April affecting the Low Countries, the London and Paris basins, Germany,  
464 Switzerland, Austria and the Czech Lands. The vine bloom ended in early June. Grapes in Beaune  
465 were picked extremely early. It didn't rain in Zürich, Switzerland, for 13 weeks. The drought lasted  
466 until November. Lake Zürich and the Rhine in Mainz dropped to very low levels. Springs and soils  
467 dried up. The Vltava river in the Czech Lands could be crossed without wetting the feet. Its water  
468 turned green, probably due to algae, which prevented people from drinking it (Pfister and Wanner,  
469 2021: 177).

470 **1420: Spring dry; summer hot, but not dry**

471 Metz (FR): Spring very warm. Soest (DE): February, March, April, May hot and dry. Basel (CH):  
472 summer drought. Lichtensteig (CH): May very hot and dry, pastures dry. Rötteln (DE): March and  
473 April very warm. Stuttgart: good weather during the year (Alexandre 1987: 568). Dry spring-summer  
474 in England (Titow 1970: 337). Drought impacts are not reported in the evidence contained in the  
475 catalogue of Alexandre (1987), and the year is not mentioned in the synthesis by Glaser and Kahle  
476 (2020) for Germany and by Brázdil et al. (2019) for the Czech Lands.

477 **1473: Spring dry; summer hot and dry**

478 The winter of 1473 was rainy in Metz (FR), and without snow and ice in Basel, Switzerland. Fruit  
479 trees began flowering in early March, which points to extremely high temperatures during the  
480 preceding weeks. April turned so hot, that vines were already in bloom at the end of this month. In  
481 May people could hardly bear the heat. Ripe grapes were found in early July. Grapes, mostly white  
482 varieties, were picked from the second half of August in many regions. Independent sources report  
483 four to five months without noteworthy precipitation. Not a drop fell in Basel from 29 June to mid-  
484 September. At that time, many trees had already dropped their leaves and looked “like at Christmas”.  
485 The Moselle being the most important western tributary of the Rhine became a trickle. Rivers in the  
486 Czech Lands, the Danube in Hungary, the Oder and Vistula in Poland, and rivers in western Russia  
487 could be forded. “Forests, woods, thickets, and forested hills burned with fire” in Poland and in  
488 Belarus. There was no way to put it out, and it was impossible to extinguish the flame before the fire  
489 devoured the roots (Przybylak et al. 2020).

490 A second flowering of fruit trees, indicating extremely high temperatures, was observed in autumn. In  
491 December, “spring-like” temperatures still prevailed and spring flowers were found. In Metz (FR) the  
492 subsequent winter of 1474 was again rainy without frost. The Basel diarist Johannes Knebel noted  
493 that even the “high mountains” – i.e. probably the peak of the Black Forest, Germany, at an altitude of  
494 1493 m – were without snow. A snowfall on 2nd March 1474, put an end to this 14-month-long warm



495 spell. Central and Eastern Europe were ravaged by wildfires. Large parts of Italy also suffered from  
496 drought, according to selective evidence. In Modena and most of the other regions of the Po Valley, it  
497 did not rain from the beginning of 1473 until March 1474. Wells within eight miles of town dried up.  
498 A lot of cattle died and grain harvests failed, which led to famine. Major swarms of locusts (*Locusta*  
499 *migratoria*) invaded Central Europe in 1474 and 1475 (Pfister and Wanner, 2021: 188).

500 **1503: May dry; summer hot and dry**

501 Temperatures in May and those in summer were extremely high in Central Europe (Dobrovolný et al.,  
502 2010). Precipitation was below average in the Czech Lands (Dobrovolny et al., 2014) and in  
503 Switzerland (<http://www.echdb.unibe.ch/selection/occ/en/pf-3458-5>). Processions for rain were held  
504 in Geneva (<http://www.echdb.unibe.ch/selection/occ/en/pf-4091-1>). In Eastern France it was the worst  
505 drought since 1473. No rain fell from early May to 12 June, when a rain spell temporarily refreshed  
506 the vegetation. Throughout the summer, the weather was so hot and dry that there was hardly any  
507 grass in the meadows. Most crops were lost due to the severe heat and drought. In many places, the  
508 vines were scorched by the dry wind, and trees such as pear and apple trees. Rivers were very low.  
509 Precipitation was more abundant in the surrounding hills, probably due to thunderstorms. Vegetables,  
510 fruit, meat and dairy products were expensive (translated from old French by Laurent Litzenburger).  
511 (Bruneau, 1933: 19, Larchey, 1857: 445f).

512 **1504: spring dry; summer hot and dry**

513 Metz (FR): No rain from April 1<sup>st</sup> to 15<sup>th</sup> June, severe damage to most cultivated crops. Subsequently  
514 intensive rain for several days". Summer: low precipitation (Prague Czech Republic). Midsummer:  
515 low water, many springs failed (Mellingen, Canton Argovia, Switzerland).

516 **1516: spring dry; summer hot and dry**

517 The winter was rainy, without snow and almost without frost  
518 (<http://www.echdb.unibe.ch/selection/occ/en/ll-0002-391>). The period from April to October was very  
519 warm and dry in Central Europe (Dobrovolný et al., 2010, 2014) and in Eastern France  
520 (<http://www.echdb.unibe.ch/selection/occ/en/ll-0004-22>). People thought that the drought was the  
521 worst since 1473 (<http://www.echdb.unibe.ch/selection/occ/en/pf-4023-3>). The wine was excellent  
522 (Pfister et al., 2024). The drought was so persistent that rivers dropped to very low levels. This made  
523 it possible to repair the bridges (Marchal, 1859). Water had to be fetched over some distance for 16  
524 weeks in the Swiss town of Winterthur. Large quantities of fish were sold at the market for a long  
525 time. Mortality was high in some regions (<http://www.echdb.unibe.ch/selection/occ/en/ll-0004-22>).

526 **1536: May dry; summer hot and dry**

527 The heat and drought began in May of this year and lasted until November, when roses were seen  
528 flowering for a second time. In August a procession for rain was held in Paris. Forest and settlement  
529 fires were frequent in Saxony, Germany, and in the Czech Lands. Cattle died from heat and  
530 starvation. Grape harvests were early, abundant and sweet. Spring, Summer and Autumn temperatures



531 were extremely high (Dobrovolný et al., 2010) Annual precipitation was very low

532 (<http://www.echdb.unibe.ch/selection/occ/en/pf-5001-142>).

533 **1540: spring dry; summer hot and dry**

534 This year was the hottest and driest in Western and Central Europe, next to 1473. Annual  
535 temperatures were the highest since 1500. The drought covered an area reaching from western France  
536 to Poland and from central Italy to northern Germany. Estimated annual precipitation both on the  
537 Swiss Plateau and in Krakow, Poland, was only about a quarter of the 20th century average. Large  
538 rivers became runnels that could be waded or crossed on horseback, while smaller watercourses dried  
539 out completely. The level of Lake Constance was so low that the lake floor, with its irregular  
540 topography, was visible. Forest fires became rampant in many parts of the continent; infernos that  
541 nobody could get under control. Town fires in Germany, were more frequent in 1540 than in any other  
542 peace year since 1000 AD. Cattle all over Europe died of thirst and hunger. Transport ships carried  
543 only a fraction of their usual cargo, while many watercourses were not navigable at all (Pfister and  
544 Wanner, 2021: 199-200). In 1546/ and 1547, the Czech Lands and Lower Austria were ravaged by  
545 locust invasions (Brázdil et al., 2014, pp. 348–349, Rohr, 2019).

546 **1559: spring dry; summer hot, but not dry**

547 April was quite warm and rather dry in Central Europe  
548 (<http://www.echdb.unibe.ch/selection/occ/en/pf-4097-577>), the Swiss precipitation Index was  
549 moderately dry (-0.67) while the Czech Lands were extremely dry  
550 (<http://www.echdb.unibe.ch/selection/occ/en/pf-5001-233>. Summer was warm in Central Europe  
551 (Dobrovolný et al., 2010), with Switzerland experiencing a moderately dry season.  
552 (<http://www.echdb.unibe.ch/selection/occ/en/pf-4046-3807> ) From 18 July onwards, it became so hot  
553 that grapes stopped growing in many places. Everyone was longing for rain. A period of rain began on  
554 18 September (<http://www.echdb.unibe.ch/selection/occ/en/pf-3168-4>). Precipitation was low in the  
555 Czech lands, but this year is not listed among the droughts in Germany (Glaser and Kahle, 2020) and  
556 in the list by Brázdil et al. (2019).

557 **1590: spring variable; summer hot and dry**

558 This extremely hot and dry summer is atypical, because it was not preceded by a warm and dry  
559 spring. April was rather warm in Central Europe, but May was cold (Dobrovolný et al., 2010) and the  
560 first weeks in June were rainy in Switzerland . The heatwave only began in the last week of June  
561 lasting until the end of August. Water became scarce in the Alps, because not even a drop of dew fell,  
562 as had been the case during the scorching summer of 1540, as the painter and schoolteacher Hans  
563 Ardüser from the Swiss Canton Grisons reports ([http://www.echdb.unibe.ch/selection/occ/en/pf-3177-  
564 37](http://www.echdb.unibe.ch/selection/occ/en/pf-3177-37)). In Slany, in the Czech Lands, no rain fell between 3 June and 21 September. The level of the  
565 Elbe and Vltava rivers was low, and the soil dried out to dust which made sowing in autumn difficult.  
566 Harvests were poor in the Czech Lands (Brazdil et al., 2019). In Poland the drought lasted from the



567 end of May to the end of autumn. The Odra river became so shallow that it could be crossed. The  
568 river mills stopped working (Przybylak et al., 2020).

569 **1603: spring dry; summer hot, but not dry**

570 Spring was mainly dry in Switzerland (<http://www.echdb.unibe.ch/selection/occ/en/pf-5006-10>).  
571 Lucerne scientist Renward Cysat reported that it had never rained much before 6 May that year  
572 (<http://www.echdb.unibe.ch/selection/occ/en/pf-2332-327>). He recorded nine very hot days in June,  
573 whereby the hot spell continued into early July (<http://www.echdb.unibe.ch/selection/occ/en/pf-2332-333>). The first ripe grapes appeared in early July (<http://www.echdb.unibe.ch/selection/occ/en/pf-2332-332>). In August, Cysat recorded 21 hot days, albeit it snowed in the Alps on the 13th of this month.  
574 332). In August, Cysat recorded 21 hot days, albeit it snowed in the Alps on the 13th of this month.  
575 332). In August, Cysat recorded 21 hot days, albeit it snowed in the Alps on the 13th of this month.  
576 <http://www.echdb.unibe.ch/selection/occ/en/pf-2332-328>). Autumn was warm, with fruit trees  
577 blooming a second time, whereby the fruit did not ripen. The warm weather continued into winter  
578 (<http://www.echdb.unibe.ch/selection/occ/en/pf-2332-323>). In Germany, thunderstorms were frequent  
579 (Glaser, 2001). 1603 is not recorded as a drought year in Germany (Glaser and Kahle, 2020), nor in  
580 the Czech Republic (Brázdil et al., 2019).

581 **1616: spring dry; summer hot and drought spatially different**

582 This drought mainly affected eastern Central Europe. In Germany, the warm, dry conditions began in  
583 mid-April. Tree rings indicated a 40% precipitation deficit for spring and summer. In Switzerland, no  
584 rain was reported during the 54-day period between 6 June and 30 July. In the Czech Lands, the  
585 drought began in April or May and lasted until late December. The soil dried out, pastures and  
586 meadows withered and spring crops failed. The “hunger stone” on the left bank of the Elbe near Děčín  
587 commemorates this disaster. Central European temperatures were 2.7 °C ( $\pm 0.49$  °C) above the 1961–  
588 90 average (Pfister and Wanner, 2021: 212).

589 **1638: spring dry, summer rather warm, but not dry**

590 April and May were extremely warm in Central Europe, which spurred vegetation growth  
591 (Dobrovolný et al., 2010). Spring was dry in the Czech Lands, but no impact is mentioned. June and  
592 July were rather warm in Central Europe (Dobrovolný et al., 2010), and dry in the Czech Lands  
593 (Dobrovolný et al., 2014).

594 **1684: May dry; summer hot and dry outside the Alps**

595 Spring was extremely dry in Prague and Zurich, accompanied by above-average temperatures in Paris  
596 and average temperatures in Central Europe. March was cold there, April was average, and May was  
597 extremely warm and dry (Rousseau, 2009). The summer was extremely hot in Paris and Central  
598 Europe and extremely dry in Zurich and Prague. Very high temperatures were recorded in June and  
599 August, while July was somewhat cooler. There was a lot of rain in the Swiss mountains. A heatwave  
600 with northeasterly winds set in for about five months from early May. Prayers for rain were already  
601 being held in Germany in May. Grain crops suffered in the Czech Lands. Bush and forest fires were  
602 rampant. The sun turned blood red behind a veil of stinking, dry fog, probably caused by forest fire



603 aerosols. Many trees in London dropped their leaves (Pfister and Wanner, 2021: 213). Water  
604 reservoirs dried up in Poland. The drought destroyed grain and flax, and grass turned to ash. Cattle  
605 died due to a lack of grass and water. The drought began at the end of June and continued until  
606 September (Pzybylak et al., 2020).

607 **1686: spring dry, summer average**

608 Spring was very warm and dry in Central Europe (Dobrovolný et al., 2010, 2014) and rather warm in  
609 Paris (Rousseau, 2009). This was mainly due to very high temperatures in May following average  
610 temperatures in April. In Paris the season was rather warm (Rousseau, 2009). Summer temperatures  
611 were average in Central Europe and drought impacts are not mentioned.

612 **1706: Spring dry; summer hot and dry**

613 Spring (mainly April) was dry in Zürich according to the number of rain days  
614 (<http://www.echdb.unibe.ch/selection/occ/de/pf-4067-28>) and in Paris based on instrumental  
615 measurements (Slonosky, 2002). Drought impacts are mentioned for Germany in Glaser and Kahle,  
616 2020, and for the Czech Lands (Brázdil et al., 2019).

617 **1719: Spring dry; summer hot and dry**

618 May was extremely dry in Zürich and Paris (MAM) based on instrumental measurements (Pfister,  
619 1978, Slonosky 2002). Drought impacts are mentioned in Glaser and Kahle (2020), in the Czech  
620 Lands (Brázdil et al., 2019) and in Europe (Pfister and Wanner, 2021: 225).

621 **1947: spring dry: summer hot, dry from late summer**

622 Spring temperatures in Central Europe were 1.4 °C above the 1961–90 average,. The season was dry  
623 on the Swiss Plateau and extremely dry in the Czech Lands. Summer temperatures were 1.9 °C above  
624 the 1961–90 average (Dobrovolný et al., 2010; Dobrovolný 2014). In general, precipitation deficits  
625 were larger in the Czech Lands than in the Swiss Plateau. In the Czech Lands, the 1947 event was one  
626 of the three most significant hydrological drought episodes since the late 1880s. Harvests of cereals  
627 and other agricultural crops were very low. River Elbe discharges at Decín were 50% below the long-  
628 term mean. The agricultural drought mainly affected fodder crops, wheat and potatoes (Brazdil et al.,  
629 2016).

630 In Switzerland, the drought only became noticeable as the summer progressed. When water levels  
631 reached their lowest point in September and October, shipping on the Rhine below Basel was  
632 suspended. Smaller rivers dried up much more severely. In autumn, the city of Bern's drinking water  
633 supply reached its capacity limit. In agriculture, the drought had the most severe impact on fodder  
634 production (Schorer, 1992). In many ways, the drought in 1947 appears to be in many ways quite  
635 similar to 1590. Several of the above mentioned historical droughts, were longer lasting and more  
636 severe than the event in 1947, in particular the mega droughts in 1473 and 1540.

637



638 **References**

- 639 Alexandre, P.: *Le climat en Europe au Moyen Âge. Contribution à l'histoire des variations climatiques de 1000*  
640 *à 1425, d'après les sources narratives de l'Europe occidentale*. Éditions de l'École des Hautes Études en Sci-  
641 ences Sociales, Paris, 1987.
- 642 Böhnisch, A., Felsche, E., Mittermeier, M., Poschlo, B., and Ludwig, R.: Future patterns of compound dry and  
643 hot summers and their link to soil moisture droughts in Europe. *Earths Future*, 13,  
644 <https://doi.org/10.1029/2024EF004916>, 2025.
- 645 Brázdil, R., Řezníčková, L., Valášek, H., Kiss, A., and Kotyza, O.: Past locust outbreaks in the Czech Lands: do  
646 they indicate particular climatic patterns?, *Theor. Appl. Climatol.*, 116, 343–357,  
647 <https://doi.org/10.1007/s00704-013-0950-9>, 2014.
- 648 Brázdil, R., Raška, P., Trnka, M., Zahradníček, P., Valášek, H., Dobrovolný, P., Řezníčková, L., Treml, P., and  
649 Stachon, Z.: The Central European drought of 1947: causes and consequences. *Clim. Res.*, 70, 161–178,  
650 <https://doi.org/10.3354/cr01387>, 2016.
- 651 Brázdil, R., Demarée, G. R., Kiss, A., Dobrovolný, P., Chromá, K., Trnka, M., Dolák, L., Řezníčková, L., Zah-  
652 radníček, P., Limanowka, D., and Jourdain, S.: The extreme drought of 1842 in Europe as described by both  
653 documentary data and instrumental measurements. *Clim. Past*, 15, 1861–1884, [https://doi.org/10.5194/cp-15-](https://doi.org/10.5194/cp-15-1861-2019)  
654 [1861-2019](https://doi.org/10.5194/cp-15-1861-2019), 2019.
- 655 Brönnimann, S., Franke, J., Valler, V., Hand, R., Samakinwa, E., Lundstad, E., Burgdorf, A.-M., Lipfert, L.,  
656 Pfister, L., Imfeld, N., and Rohrer, M.: Past hydroclimate extremes in Europe driven by Atlantic Jet stream and  
657 recurrent weather patterns. *Nature Geoscience*, 18, 246–253, <https://doi.org/10.1038/s41561-025-01654-y>, 2025.
- 658 Bruneau, C.: *La Chronique de Philippe de Vigneulles*. Société d'histoire et d'archéologie de la Lorraine, Metz,  
659 1933.
- 660 Buisman, J.: *Duizend jaar weer, wind en water in de Lage Landen, II, 1300-1450* (ed. van Engelen, A. F. V.),  
661 1996.
- 662 Cleveland, W. S.: Robust locally weighted regression and smoothing scatterplots. *J. Am. Stat. Assoc.*, 74, 829–  
663 836, <https://doi.org/10.2307/2286407>, 1979.
- 664 Cook, B. I., Smerdon, J. E., Cook, E. R., Williams, A. P., Anchukaitis, K. J., Mankin, J. S., et al.: Megadroughts  
665 in the Common Era and the Anthropocene. *Nature Reviews Earth & Environment*, 1–17, 2022.
- 666 Dobrovolný, P., Brázdil, R., Trnka, M., Kotyza, O., and Valášek, H.: Precipitation reconstruction for the Czech  
667 Lands, AD 1501–2010. *Int. J. Climatol.*, <https://doi.org/10.1002/joc.3957>, 2014.
- 668 Dobrovolný, P., Moberg, A., Brázdil, R., Pfister, C., Glaser, R., and Böhm, R.: Monthly, seasonal and annual  
669 temperature reconstructions for Central Europe since AD 1500. *Clim. Change*, 101, 69–107, 2010.
- 670 Fischer, E. M., Seneviratne, S. I., Lüthi, D., and Schär, C.: Contribution of land–atmosphere coupling to recent  
671 European summer heat waves. *Geophys. Res. Lett.*, 34, <https://doi.org/10.1029/2006GL029068>, 2007.
- 672 Glaser, R.: *Klimageschichte Mitteleuropas*. Primus Verlag, Darmstadt, 2001.
- 673 Glaser, R. and Kahle, M. O.: Reconstructions of droughts in Germany since 1500. *Clim. Past*, 16, 1207–1222, ,  
674 2020.



- 675 Hand, R., Samakinwa, E., Lipfert, L., and Brönnimann, S.: ModE-Sim – a medium-size AGCM ensemble to  
676 study climate variability during the past 600 years. *Geosci. Model Dev.*, 16, 4853–4866,  
677 <https://doi.org/10.5194/gmd-16-4853-2023>, 2023
- 678 Hersbach, H., Bell, B., Berrisford, P., et al.: The ERA5 global reanalysis. *Q. J. R. Meteorol. Soc.*, 146, 1999–  
679 2049, <https://doi.org/10.1002/qj.3803>, 2020.
- 680 Hirschi, M., Seneviratne, S. I., Alexandrov, V., et al.: Observational evidence for soil-moisture impact on hot  
681 extremes in southeastern Europe. *Nat. Geosci.*, 4, 17–21, <https://doi.org/10.1038/ngeo1032>, 2011.
- 682 IPCC: *Climate Change 2021: The Physical Science Basis*. Cambridge University Press,  
683 <https://doi.org/10.1017/9781009157896>, 2021.
- 684 Jungclaus, J. H., et al.: The PMIP4 contribution to CMIP6 – Part 3: The last millennium. *Geosci. Model Dev.*,  
685 10, 4005–4033, <https://doi.org/10.5194/gmd-10-4005-2017>, 2017.
- 686 Labbé, T., Pfister, C., Brönnimann, S., Rousseau, D., Franke, J., and Bois, B.: The longest homogeneous series  
687 of grape harvest dates. *Clim. Past*, 15, 1485–1501, <https://doi.org/10.5194/cp-15-1485-2019>, 2019.
- 688 Larchey, L.: *Journal de Jehan Aubrion, bourgeois de Metz, avec sa continuation par Pierre Aubrion (1465–*  
689 *1512)*. Metz, 1857.
- 690 Lipfert, L., Hand, R., and Brönnimann, S.: A global assessment of heatwaves since 1850. *Geophys. Res. Lett.*,  
691 51, <https://doi.org/10.1029/2023GL106212>, 2024.
- 692 Lipfert, L., Hand, R., and Brönnimann, S.: Comparing 600 years of extremely hot Central European summers to  
693 future projections. *Sci. Rep.*, <https://doi.org/10.1038/s41598-026-45507-z>, 2026.
- 694 Marchal, L.: *La Chronique de Lorraine*. Société d’Archéologie Lorraine, Nancy, 5, 336 pp., 1859.
- 695 McVicar, T. R., Roderick, M. L., Donohue, R. J., Li, L. T., Van Niel, T. G., Thomas, A., Grieser, J., Jhajharia,  
696 D., Himri, Y., Mahowald, N. M., Mescherskaya, A. V., Kruger, A. C., Rehman, S., and Dinpashoh, Y.: Global  
697 review and synthesis of trends in observed terrestrial near-surface wind speeds: Implications for evaporation. *J.*  
698 *Hydrol.*, 416–417, 182–205, 2012.
- 699 Pardo, S. K. and Paredes-Fortuny, L.: Uneven evolution of regional European summer heatwaves under climate  
700 change. *Weather Clim. Extremes*, 43, 100648, <https://doi.org/10.1016/j.wace.2024.100648>, 2024.
- 701 Pfister, C.: Climate and economy in eighteenth-century Europe. *J. Interdiscip. Hist.*, 9, 223–243, 1978.
- 702 Pfister, C., Rohr, C., and Jover, A. C. C.: Euro-Climhist: eine Datenplattform der Universität Bern zur Witte-  
703 rungs-, Klima- und Katastrophengeschichte. *Wasser Energie Luft*, 109, 45–48, 2017.
- 704 Pfister, C. and Wanner, H.: *Climate and Society in Europe*. Haupt, Bern, 2021.
- 705 Pfister, C., Brönnimann, S., Altwegg, A., et al.: 600 years of wine must quality. *Clim. Past*, 20, 1387–1399, ,  
706 2024.
- 707 Pfister, C., Brönnimann, S., Litzenburger, L., et al.: Wine must yields as indicators of climate. *Clim. Past*, 22,  
708 541–559, <https://doi.org/10.5194/cp-22-541-2026>, 2026.
- 709 Pfister, L., Wilhelm, L., Brugnara, Y., Imfeld, N., and Brönnimann, S.: Weather type reconstruction using ma-  
710 chine learning approaches. *Weather Clim. Dynam.*, 6, 571–594, <https://doi.org/10.5194/wcd-6-571-2025>, 2025.



- 711 Pliemon, T., Foelsche, U., Rohr, C., and Pfister, C.: Precipitation reconstructions for Paris based on the observa-  
712 tions by Louis Morin, 1665–1713 CE. *Clim. Past*, 19, 2237–2256, <https://doi.org/10.5194/cp-19-2237-202>,  
713 2023.
- 714 Pribyl, K.: *Farming, Famine and Plague*. Springer, Cham, 2017.
- 715 Pribyl, K., Cornes, R., and Pfister, C.: Reconstructing medieval April–July mean temperatures in East Anglia,  
716 1256–1431. *Clim. Change*, 113, 393–412, <https://doi.org/10.1007/s10584-011-0327-y>, 2012.
- 717 Pribyl, K. and Cornes, R. C.: Droughts in medieval England (Part 1). *Weather*, 75, 168–172,  
718 <https://doi.org/10.1002/wea.3599>, 2019.
- 719 Pribyl, K. and Cornes, R. C.: Droughts in medieval England (Part 2). *Weather*, 75, 196–198,  
720 <https://doi.org/10.1002/wea.3529>, 2020.
- 721 Przybylak, R., Oliński, P., Koprowski, M., Filipiak, J., Pospieszynska, A., Chorążyczewski, W., Puchałka, R.,  
722 and Dąbrowski, H. P.: Droughts in the area of Poland in recent centuries in the light of multi-proxy data. *Clim.*  
723 *Past*, 16, 627–661, <https://doi.org/10.5194/cp-16-627-2020>, 2020.
- 724 Quesada, B., Vautard, R., Yiou, P., Hirschi, M., and Seneviratne, S. I.: Asymmetric European summer heat pre-  
725 dictability from wet and dry southern winters and springs. *Nat. Clim. Change*, 2, 736–741,  
726 <https://doi.org/10.1038/nclimate1536>, 2012.
- 727 Rohr, C.: *Apocalyptic riders in the borderlands. Dealing with locust invasion, diseases and war in fifteenth- and*  
728 *sixteenth-century Eastern and Southern Austria*. In: *The Dance of Death in Late Medieval and Renaissance Eu-*  
729 *rope* (Ed. Kiss, A., and Pribyl K.), Taylor and Francis, 107–124, 2019.
- 730 Rohrer, M., Martius, O., Raible, C. C., and Brönnimann, S.: Sensitivity of blocks and cyclones in ERA5 to spa-  
731 tial resolution and definition. *Geophys. Res. Lett.*, 47, e2019GL085582, <https://doi.org/10.1029/2019GL085582>,  
732 2020.
- 733 Rousi, E., Fink, A. H., Andersen, L. S., et al.: The extremely hot and dry 2018 summer in Europe. *Nat. Hazards*  
734 *Earth Syst. Sci.*, 23, 1699–1718, <https://doi.org/10.5194/nhess-23-1699-2023>, 2023.
- 735 Rousseau, D.: Les températures mensuelles en région parisienne de 1676 à 2008. *La Météorologie*, 8e série 67,  
736 43–55, 2009.
- 737 Samakinwa, E., Valler, V., Hand, R., et al.: An ensemble reconstruction of global monthly sea surface tempera-  
738 ture and sea ice concentration 1000–1849. *Sci. Data*, 8, 261, <https://doi.org/10.1038/s41597-021-01043-1>, 2021.
- 739 Sato, M., Hansen, J. E., McCormick, M. P., and Pollack, J. B.: Stratospheric aerosol optical depths, 1850–1990.  
740 *J. Geophys. Res. Atmos.*, 98, 22987–22994, <https://doi.org/10.1029/93JD02553>, 1993.
- 741 Schorer, M.: *Extreme Trockensommer in der Schweiz und ihre Folgen für Natur und Wirtschaft*. Geographica  
742 Bernensia G40, Geographisches Institut der Universität Bern, 1992.
- 743 Seneviratne, S. I., Corti, T., Davin, E. L., et al.: Soil moisture–climate interactions. *Earth-Sci. Rev.*, 99, 125–  
744 161, 2010.
- 745 Slivinski, L. C., Compo, G. P., Whitaker, J. S., et al.: Towards a more reliable historical reanalysis: Improve-  
746 ments for version 3 of the Twentieth Century Reanalysis system. *Q. J. R. Meteorol. Soc.*, 145, 2876–2908,  
747 <https://doi.org/10.1002/qj.3598>, 2019.



- 748 Slonosky, V. C.: Wet winters, dry summers? Three centuries of precipitation data from Paris. *Geophys. Res.*  
749 *Lett.*, 29, 1887, <https://doi.org/10.1029/2001GL014302>, 2002.
- 750 Tibaldi, S. and Molteni, F.: On the operational predictability of blocking. *Tellus A*, 42, 343–365,  
751 <https://doi.org/10.3402/tellusa.v42i3.11882>, 1990.
- 752 Titchner, H. A. and Rayner, N. A.: The Met Office Hadley Centre sea ice and sea surface temperature data set,  
753 version 2: 1. Sea ice concentrations. *J. Geophys. Res. Atmos.*, 119, 2864–2889,  
754 <https://doi.org/10.1002/2013JD020316>, 2014.
- 755 Titow, J.: Evidence of weather in the account rolls of the bishopric of Winchester 1209–1350. *Econ. Hist. Rev.*,  
756 12, 360–407, 1960.
- 757 Titow, J.: Le climat à travers les rôles de comptabilité de l'évêché de Winchester (1350–1450). *Ann. Hist. Sci.*  
758 *Soc.*, 25, 312–350, <https://doi.org/10.3406/ahess.1970.422220>, 1970.
- 759 Träger-Chatterjee, C., Müller, R., and Bendix, J.: Analysis of extreme summers and prior late winter/spring con-  
760 ditions in Central Europe. *Nat. Hazards Earth Syst. Sci.*, 13, 1243–1257, [https://doi.org/10.5194/nhess-13-1243-](https://doi.org/10.5194/nhess-13-1243-2013)  
761 [2013](https://doi.org/10.5194/nhess-13-1243-2013), 2013.
- 762 Valler, V., Franke, J., Brugnara, Y., et al.: ModE-RA: a global monthly paleo-reanalysis of the modern era 1421  
763 to 2008. *Sci. Data*, 11, 36, <https://doi.org/10.1038/s41597-023-02733-8>, 2024.
- 764 Vautard, R., Yiou, P., D'Andrea, F., et al.: Summertime European heat and drought waves. *Geophys. Res. Lett.*,  
765 34, <https://doi.org/10.1029/2006GL028001>, 2007.
- 766 Wang, G., Dolman, A. J., and Alessandri, A.: A summer climate regime over Europe modulated by the North  
767 Atlantic Oscillation. *Hydrol. Earth Syst. Sci.*, 15, 57–64, <https://doi.org/10.5194/hess-15-57-2011>, 2011.
- 768 Warren, R., et al.: ClimeApp: data processing tool for monthly, global climate data from the ModE-RA palaeo-  
769 reanalysis, 1422 to 2008 CE. *Clim. Past*, 20, 2645–2662, 2024.
- 770